Official Journal Issued by Faculty of Veterinary Medicine

Benha Veterinary Medical Journal

Journal homepage: https://bvmj.journals.ekb.eg/

Since 1990

Original Paper

Prospective ameliorative activity of neem (*Azadirachta Indica*) on iron oxide nanoparticle-induced multiple organ injury via attenuating TNF-α pathway

Radwa A. M. N. Amin[1,2*], Nabila M. Abd Elaliem[1], Ahmed A. Abdeen[1], Samer S. Ibrahim[1], Moamen H. Elsafty[3], Ebtssam G. A. Beder[1]

[1] *Department of Forensic Medicine and Toxicology, Faculty of Veterinary Medicine, Benha University, Egypt.*

[2] *Menoufia University Hospital, Faculty of Veterinary Medicine, Sadat City University, Egypt.*

[3] *Department of Pharmacology, Faculty of Veterinary Medicine, Benha University, Egypt.*

ARTICLE INFO

Keywords

Fe_2O_3 NP

Histopathology

Immunohistochemistry

Neem

Received 01/03/2023
Accepted 18/03/2023
Available On-Line 01/04/2023

ABSTRACT

Neem trees *(Azadirachta indica)* have received a lot of academic interest recently because of their strong antioxidant and anti-proliferative capabilities. In this study, we evaluated the potential alleviating effect of neem on Fe_2O_3 NP -induced damage in brain, heart, and testis. Twenty-eight male albino rats were divided into four equal groups at random. The control group was given distilled water orally for 45 days, Neem group was given 200 mg/kg/day orally for 45 days, Fe_2O_3 NP group was given 60 mg/kg of Fe_2O_3 NP I/P at the 31st-45th day, Fe_2O_3 NP +Neem group was given 200 mg/kg day of neem orally for 45 days + 60 mg/kg of Fe_2O_3 NP IP at the 31st–45th day. In the present investigation, histopathological examination of brain, heart, and testis sections revealed cellular degeneration and necrosis after Fe_2O_3 NP exposure. Also, TNF-α expressions were considerably elevated. Neem pr-treatment maintained tissue architecture in Fe_2O_3 NP-intoxicated rats. Our findings proved that neem have a potential protective impact against cellular damage induced by Fe_2O_3 NP through its anti-inflammatory, antiapoptotic, and antioxidant effects.

1. INTRODUCTION

Nanotechnology is becoming a growing hazard to human existence. Materials that are nano scale (with diameters between 1 and 100 nm) can enter the human and animal bodies freely through various entrance points. After oral exposure or inhalation, circulating nanoparticles reach the liver, lungs, heart, digestive system, and brain (Hagens et al., 2007). Researchers have been concerned about the environment's and people's exposure to nanoparticles (NPs) toxicity and this concern still requires elucidation.

Iron oxide nanoparticles (Fe_2O_3 NP) have recently gained significant attention in a variety of clinical and medical applications including nano medicines, drug targeting, drug delivery, tissue healing, and magnetic hyperthermia in cancer treatment (Dadfar et al., 2019). In vivo investigations have demonstrated that Fe_2O_3 NP enter cells, reside in cell organelles (endosomes/lysosomes), decompose, and contribute to the cellular iron pool before being released into the cytoplasm. Magnetic Fe_2O_3 NP can build up in liver, lungs, brain, and etc., where they can lead to inflammation, tissue necrosis, and disturbed blood coagulation (Zhu et al., 2008). Reactive oxygen species (ROS) production and programmed cell death are two of the fundamental processes that underlie the Fe_2O_3 NP induced toxicity (Liu et al., 2013). Therefore, according to some authors' theories, antioxidants should be one of the key elements of a successful treatment strategy for Fe_2O_3 NP -induced toxicity (Missaoui et al., 2018).

Numerous studies have been conducted on plants because of their positive benefits on health, *Azadirachta indica* (also known as Neem; A. indica) has been utilized as food and a folk remedy. Neem leaf extracts have been discovered to have immune-modulatory, anti-inflammatory, anti-genotoxic, and anti-carcinogenic effects. Their effects are caused by an up regulation of antioxidant defenses and scavenging free radical (Subapriya et al., 2006). Although some chemicals from neem leaves have been shown to have therapeutic value, the majority of the pharmacological characteristics have only been described for crude extracts (Vinothini et al., 2009).

Therefore, the current investigation was designed to study the impacts of neem leaves against Fe_2O_3 NP-induced pathological alterations on brain, heart, and testis of rats.

2. MATERIAL AND METHODS

2.1. Chemicals

Iron Oxide Nano Particle (Fe_2O_3 NP), (60mg/Kg IP administration), was prepared in Future University, Egypt (Ali et al., 2016). Neem, (200 mg/kg oral administration) was bought as vegetarian capsules from ORGANIC INDIA Pvt. Ltd. (Barabanki, India).

2.2. Experimental design

Twenty-eight male albino rats with a weight of 190 ± 10 g were derived from the Egyptian Organization for Biological Products and Vaccines. All animals were kept at a

* Correspondence to: radwaaminnasef32@gmail.com

temperature of 25 ± 2 °C, had unrestricted access to commercial pellets and water, were subjected to a 12:12 h light/dark cycle and left for seven days to acclimatize before the trial. The experimental rats followed the instructions for the care and use of laboratory animals that were ethically approved by the Research Ethical Committee of the Faculty of Veterinary Medicine, Benha University, Egypt (Approval No. BUFVTM 04-11-22). Rats were weighed weekly and split at random into four equal groups as follows:

• Control group: 7 rats were given distilled water orally for 45 days.

• Neem group: 7 rats were given 200 mg/kg b.wt. per day of neem dissolved in D.W orally for 45 days (Oyagbemi et al., 2018; Gheni et al., 2020).

• Fe_2O_3 NP group: 7 rats were given distilled water orally for 45 days and Fe_2O_3 NP 60mg/kg b.wt. per day IP from the 31st day to the 45th day (Verma et al., 2021; Balas et al., 2021).

• Fe + Neem group:7 rats were given 200 mg/kg b.wt. per day of neem dissolved in D.W orally for 45 days and Fe_2O_3 NP 60 mg/kg b.wt. per day IP from the 31st day to the 45th day and kept as Co-treated group.

All groups received treatments as described above at 10 AM and observed daily. One day following the last dose, isoflurane 100% was used to anesthetize rats.

2.3. Histopathological and immunohistochemical technique

Immediately after the anesthesia, brain, heart, and testicular specimens were collected from each rat was preserved quickly in 10% neutral-buffered formalin. Then gradually dehydrated in alcohol, cleared in xylol, embedded in paraffin, sectioned at 5-µm thickness, and stained with (H&E) for histopathological examination according to the method described by Bancroft et al. (2008). Finally, light microscopy was used to examine these tissue sections (Leica, Germany). Immunohistochemical examination was performed using tumor necrosis factor alpha (TNF-α) according to Deguchi et al. (1996). Brown staining was seen on positive antigens under light microscopy. Using ImageJ software (National Institutes of Health, Bethesda, MD, USA) version 1.48. we assessed immunoreactive areas (μm^2) in ten different microscopic fields. Based on the integrated density of the positive cells, expression levels were estimated.

2.4 Statistical analysis

Statistical analysis was completed using SPSS (Version 20; SPSS Inc., Chicago, USA). One-way ANOVA was used to investigate the substantial divergence found through multiple group comparisons and The Duncan test was used as a post hoc assessment. It expresses all values as mean ± SE, with significance considered at $P \leq 0.05$.

3. RESULTS

3.1 Histopathological findings

3.1.1 Cerebrum

The microscopic examination of the cerebral cortex in control and neem groups revealed normal histological structure of these cortex which covered with thin pia mater, outer molecular layer, and many layers of pyramidal cells (Fig. 1A-B). In contrast, the examined cerebral cortex in Fe_2O_3 NP group, revealed congestion of blood vessels in pia mater with the presence of vacuolar spaces around the pyramidal cells, and degenerated neurons with pyknotic nuclei (Fig. 1C). While the examined cerebral cortex of rats in Fe + Neem group showed mild congestion of blood vessels in pia mater with the presence of fewer degenerated cells (Fig. 1D).

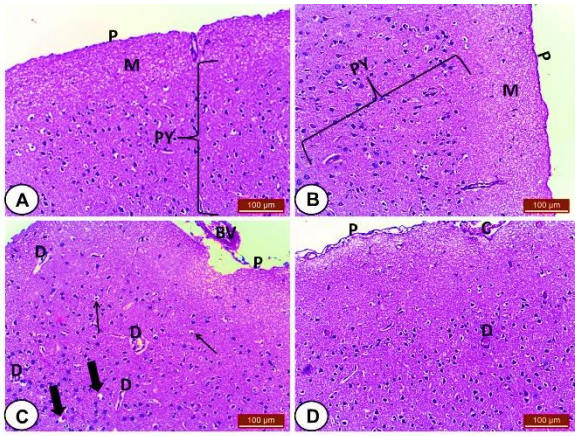

Fig. 1. Histological sections of cerebrum. A and B; Control, and Neem groups showing normal arrangement of pia mater (P), molecular layer (M) and layers of pyramidal cells (PY). C: Fe_2O_3 NP group showed congestion of the cortical blood vessels (BV), degenerated neurons with pyknotic nuclei (arrows), vacuolar spaces around the pyramidal cells (Thick arrows). D: Fe +Neem groups showed mild congestion (C) of blood vessels in pia mater (P). H&E stain, scale bars=100µm.

3.1.2 Cerebellum

Microscopically the cerebellar cortex from control and neem groups were arranged into molecular, Purkinje cell then granular layers and covered with pia Mater (Fig. 2A-B). The examined cerebellum of rats in Fe_2O_3 NP group showed marked congestion of blood vessels of pia mater with vacuolation of and degeneration of some Purkinje cells (Fig. 2C). Meanwhile only slight congestion of pia mater and medullary blood vessels was seen in Fe + Neem group (Fig. 2D).

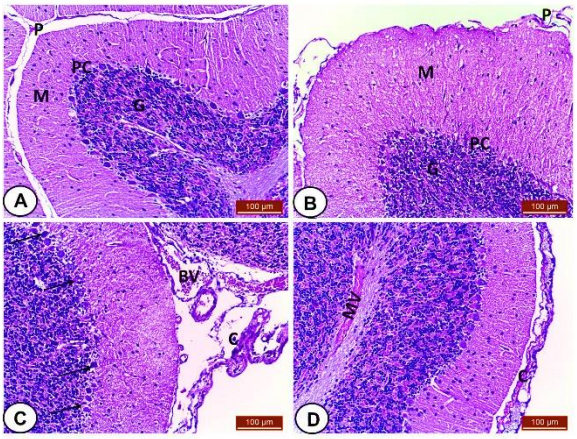

Fig. 2. Histological sections of cerebellum. A and B; Control, and Neem groups showing molecular (M), Purkinje cell (PC) and granular (G) layers of the cerebellar cortex that was covered by pia mater (P). C; Fe_2O_3 NP group showing marked congestion (C) of blood vessels (BV) in pia mater, vacuolation and degeneration of some Purkinje cells (arrows). D: Fe +Neem groups showed slight congestion (C) of pia mater and medullary blood vessels (MV). H&E stain, scale bars=100µm.

3.1.3 Heart

The examined heart of control and neem groups showed anastomosing myocardial fibers with acidophilic striated sarcoplasm, and vesicular nucleus (Fig. 3A-B). However, the heart of rats from Fe_2O_3 NP group revealed fragmented myocardial fibers with pale acidophilic sarcoplasm, pyknotic nuclei, focal areas of hyalinization and hemorrhage in between myocardial fibers (Fig. 3C). Neem pretreatment in Fe +Neem group revealed little protective effect against

the myocardial lesions induced by Fe_2O_3 NP. where some myocardial fibers demonstrated few hyalinization areas, and other showed pale acidophilic sarcoplasm with no evidence to hemorrhage (Fig. 3D).

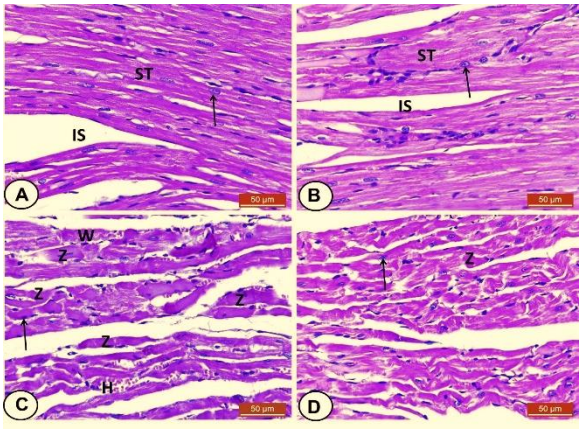

Fig. 3. Histological sections of cardiac tissue. A and B; Control, and Neem groups showing anastomosing myocardial fibers which had acidophilic striated (ST) sarcoplasm with vesicular nucleus (arrow) with interstitial spaces (IS). C; Fe_2O_3 NP group showing fragmented fibers with pale acidophilic sarcoplasm, pyknotic nuclei (arrow), focal areas of hyalinization (Z), wavy fibers (W), hemorrhage (H). D; Fe +Neem group showing few hyalinization areas (Z) and vesicular nuclei in other myocardial fibers (arrow). H&E stain, scale bars=50µm.

3.1.4 Testis

The histological examination of testis of rats from control and neem groups showed the normal histological structure of seminiferous tubules, normal arrangement of spermatogenic cells, and normal interstitial tissue (Fig. 4A-B). Meanwhile in Fe_2O_3 NP group the examined testis demonstrated marked degenerative changes and disrupted testicular architecture including vacuolation of spermatogonia, degeneration of spermatocytes, sloughing off germ cells in the lumens of seminiferous tubes interstitial edema (Fig. 4C). Fe +Neem group showed an improvement of the microscopic picture of the examined testis where only, thickened interstitial tissue and presence of germ cells in the lumen were noted (Fig. 4D).

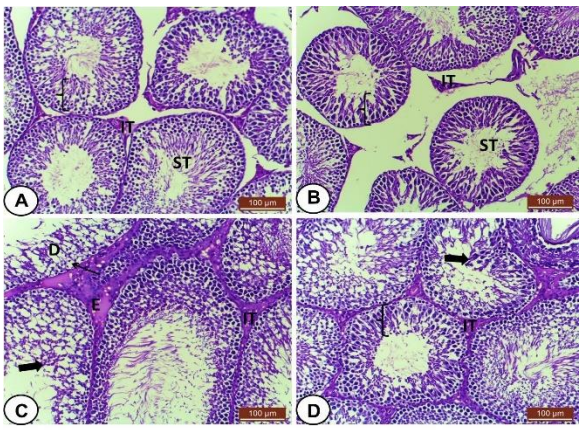

Fig. 4. Histological sections of testicular tissue. A; Control group showing normal seminiferous tubules (ST) with arrangement of spermatogenic cells (brackets) and normal interstitial tissue (IT). B; Neem group showing a wide separation between tubules. Change with another one and few mature sperm in tubules. C; Fe_2O_3 NP group showing degeneration of spermatogonia (thin arrow) (D), exfoliation of multinucleated germ cells into the lumen (thick arrows) and widening of interstitium (IT) with hemolysis. D; Fe+ Neem group showed an improvement of the microscopic picture of the examined testis where only thickened interstitial tissue and presence of germ cells in the lumen were noted. H&E stain, scale bars=100µm

3.2 Immunohistochemical analyses of the expression of TNF- α

3.2.1 Brain

Immunohistochemical staining for TNF-α showed intense immunoreaction in the brain of rats in Fe_2O_3 NP group while control and neem groups showed no evidence of TNF-α expression. The reaction was visualized as dark brown cytoplasmic granules. In Fe +Neem group, there were decreases in brownish color indicated decreased expression of TNF-α in the brain. In addition, pretreatment with neem significantly reduced TNF-α expression (Fig. 5).

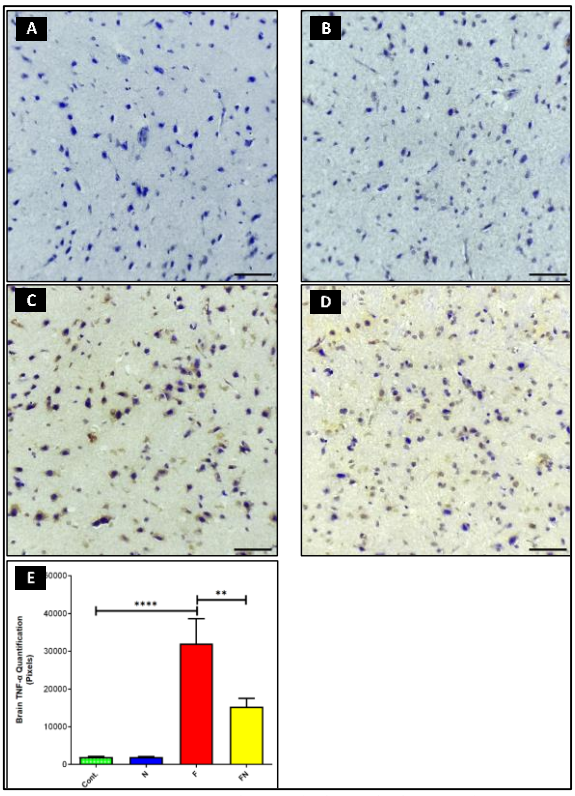

Fig. 5. Immunohistochemistry of TNF-α in the cerebral cortex of brain tissues. (A) Control group showing negative expression; (B) Neem group with negligible TNF-α expression; (C) Fe_2O_3 NP group showing intense of positive immunostaining; (D) Fe +Neem group showing weak immunostaining reaction; (E) Bars show quantification of TNF-α expression in each group

3.2.2 Heart

Immunostaining for TNF-α in the hearts of rats in Fe_2O_3 NP group revealed strong immunoreactivity compared to the control group. However, weak to moderate of staining TNF-α were seen in the Fe + Neem group. Moreover, administration of neem significantly decreased the expression of this cytokine (Fig. 6).

3.2.3 Testis

Minimal TNF-α immunoreaction in the cells of the seminiferous tubules was observed in both the control and neem groups. In the Fe_2O_3 NP group, intense TNF-α expression was observed in the interstitial areas of testis. In Fe +Neem group, decreases in expression of TNF-α were recorded with neem administration (Fig. 7).

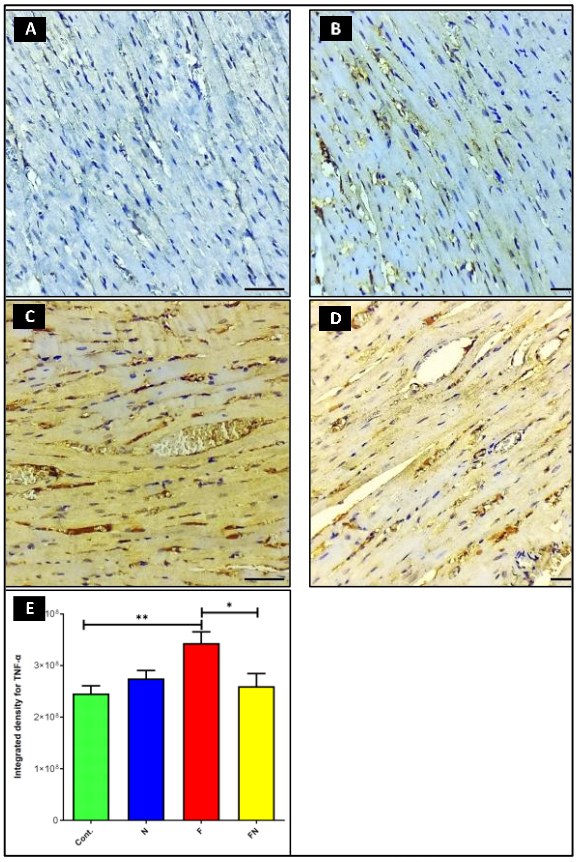

Fig. 6. Immunohistochemistry of TNF-α in myocardial tissues. (A) Control group showing unremarkable expression; (B) Neem group with weak faint TNF-α expression; (C) Fe_2O_3 NP group showing moderate expression; (D) Fe +Neem group showing mild brown staining; (E) Bars show quantification of TNF-α expression in each group.

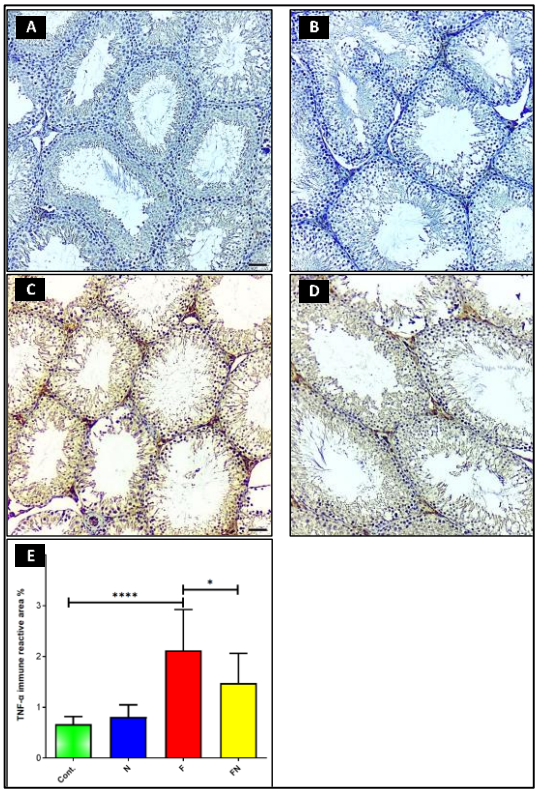

Fig. 7. Immunohistochemistry of TNF-α in rat testicular tissue. (A) control group with nominal TNF-α expression; (B) Neem group with negligeable TNF-α expression; (C) Fe_2O_3 NP group showing a significant elevation of TNF-α reactivity in interstitial areas; (D) Fe +Neem, showed mild TNF-α positivity; (E) Bars show quantification of TNF-α expression in each group.

4. DISCUSSION

Nanoparticles may either intentionally or unintentionally, have hazardous consequences on people and the environment (Li et al., 2003).

Due to their tiny size, nanoparticles can cause toxicity when they enter the human body through a variety of routes, including ingestion, inhalation, skin contact, and injection. Nanoparticles are rapidly contacted by immune cells and plasma proteins after entering the circulation. Several pathways may lead to the absorption of a nanoparticle. These pathways involve a variety of processes, such as a decrease in the number of blood cells, anti-mitotic properties, development of oxidative stress, reduction in cellular antioxidants, and a rise in the number of immune-system cells (Gaharwar et al.,2015).

In the present study, the alterations of histological structures of different organs under experiment especially the development of cytoplasmic degeneration suggesting oxidative damage caused by Fe_2O_3 NP via interacting with cellular proteins and enzymes that interfering with the antioxidant defense system, causing the production of ROS which in turn induces cellular degenerative changes (Abdelhalim et al., 2012). Also, Estelrich et al. (2015) stated that the NPs toxicity may be due to the oxidative stress and inflammatory response.

Regarding to the effect of Fe_2O_3 NP on cerebrum the result showed severe histological changes in cerebral architecture after Fe_2O_3 NP exposure that was previously reported by (Yousef et al., 2019b). Our study revealed similar findings to Yousef et al. (2019b) including vacuolar gaps surround the pyramidal cells and degenerated neurons with pyknotic nucleus and dilatation of blood vessels moreover, congestion of the cortical blood vessels and pia mater. While histopathological examination of cerebellum of rats in Fe_2O_3 NP group, showed congestion of cerebellar blood vessels in addition to marked vacuolation and degeneration of Purkinje cells. the same result was recorded by (Elshama et al., 2017; Abdel-Aziz et al., 2019) that zinc oxide nanoparticles induced perineuronal vacuoles surrounding Purkinje cells and had pyknotic nuclei. Regarding the vacuolar appearance of cytoplasm of neuronal cells in both cerebrum and cerebellum, it could be the result of cellular swelling caused by the failure of the plasma membrane's energy-dependent Na+ K+ ion pumps as a result of lipid peroxidation (Kumar et al., 2014).

Regarding to the effect of Fe_2O_3 NP on heart tissue, the microscopic examination revealed severe toxic effect on myocardial fibers. Most fibers were fragmented with pale acidophilic sarcoplasm and pyknotic nuclei. In addition, focal areas of hyalinization and hemorrhage in between myocardial fibers were noted. Such findings matched with Yousef et al. (2019a) who used Fe_2O_3 NP.

Regarding impact of Fe_2O_3 NP on testicles, the seminiferous tubules were represented by degeneration and sloughing of spermatogenic cells in addition to interstitial edema. These findings were in close to Sundarraj et al. (2017) who reported a toxic effect of Fe_2O_3 NP on testicular tissues. Finally, the histological alterations identified in the current study indicated that Fe_2O_3 NP can induce neuro, cardio, and testicular toxicity.

However, neem administration can ameliorate the structural damages induced by Fe_2O_3 NP in the different organs that might be due to its antioxidant properties (Sithisarn et al., 2005) through scavenging free radical caused by its flavonoids, nimbosterol, and limonoids (Prashanth and Krishnaiah, 2014) in addition to, its phenylpropanoids and tannins (Pokhre et al., 2015).

Tumor Necrosis Factor alpha (TNF-α) is generated by macrophages and monocytes during acute inflammation. It is in charge of a wide variety of cell signaling events that result in necrosis (Idriss et al., 2000). The present immunohistochemical study showed that Fe_2O_3 NP caused an elevation in expression of TNF-α with in cerebral cortex sections when compared with the control group which could be explained by oxidative stress which matched with Gaharwar et al. (2020) who established that Fe_2O_3 NP causes an inflammatory response as seen by an increase in TNF-α and other pro-inflammatory cytokines in serum.

In the present study, the evaluation of local proinflammatory cytokines production in the cardiac tissue by immunostaining demonstrated that as compared to the control group, the Fe_2O_3 NP group revealed intensive immunostaining for the inflammatory markers TNF-α. This data was parallel with Yousef et al. (2019a) who demonstrated that exposure to Fe_2O_3 NP led to considerably more TNF-α being produced in heart and pulmonary tissues. A similar pattern of immunohistochemical results was observed in the examined testis of rats in Fe_2O_3 NP group, where intense TNF-α expression was recorded in the interstitial areas of the testicular tissue. Numerous pro-inflammatory genes, including TNF-α may be upregulated by NPs (Khanna et al., (2015). This finding suggested that NPs could contribute to inflammation and ROS produced by the inflammation may induce DNA damage and apoptosis.

However, neem administration can ameliorate the structural damages induced by Fe_2O_3 NP in the different organs that might because it has a function in lowering pro-inflammatory cytokines including TNF-α. Morris et al. (2019) showed that neem leaf significantly reduced inflammatory marker TNF-α in vitro and in vivo. This result was inferred from ability of neem to lower pro-inflammatory cytokines including TNF-α.

5. CONCLUSION

This study concluded that Fe_2O_3 NP caused damage to several organs including brain, heart, and testis and neem mitigated these toxic effects through attenuation of TNF-α pathways.

ACKNOWLEDGMENT

The authors acknowledge Veterinary Forensic Medicine and Toxicology Department, Faculty of Veterinary Medicine, Benha University, Egypt for providing all the facilities necessary to for this work. We appreciate Dr. Mohamed M.S Gab-Allah, lecturer of Pathology, Department of Pathology, Faculty of Veterinary Medicine, Benha University for his efforts on the immunohistochemistry analysis.

6. REFERENCES

1. Abdel-Aziz HM, Mekawy NH, Ibrahem NE (2019). Histological and immunohistochemical study on the effect of zinc oxide nanoparticles on cerebellar cortex of adult male albino rats. The Egyptian Journal of Histology; 42(1): 23-34.
2. Abdelhalim, M A K, Jarrar B M (2012). Histological alterations in the liver of rats induced by different gold nanoparticle sizes, doses and exposure duration. Journal of Nanobiotechnology; 10(1): 1-9.
3. Ali A, Zafar H, Zia M, ul Haq I, Phull A R, Ali J S, Hussain A (2016). Synthesis, characterization, applications, and challenges of iron oxide nanoparticles. Nanotechnology, Science and Applications; 9:49-67.
4. Balas, M, Popescu Din, I M, Hermenean, A, Cinteza, L O, Dinischiotu, A (2021). Exposure to iron oxide nanoparticles coated with phospholipid-based polymeric micelles induces renal transitory biochemical and histopathological changes in mice. Materials; 14(10): 2605-2619.
5. Bancroft, J D, Gamble M (2008). Theory and practice of histological techniques. 6th Ed. Elsevier health sciences, Churchill Livingstone, China.
6. Dadfar SM, Roemhild K, Drude NI, Von Stillfried S, Knüchel R, Kiessling F, Lammers T (2019). Iron oxide nanoparticles: diagnostic, therapeutic and theranostic applications. Advanced Drug Delivery Reviews; 138: 302-325.
7. Deguchi, K, Mizuguchi M, Takashima S (1996). Immunohistochemical expression of tumor necrosis factor α in neonatal leukomalacia. Pediatric Neurology; 14(1): 13-16.
8. Elshama SS, El-Kenawy AEM, Osman HEH (2017). Histopathological study of zinc oxide nanoparticle induced neurotoxicity in rats. Toxicology; 13: 95-103.
9. Estelrich J, Sánchez-Martín MJ, Busquets MA (2015). Nanoparticles in magnetic resonance imaging: from simple to dual contrast agents. Int J Nanomedicine; 10:1727–1741.
10. Gaharwar, U S, Kumar S, Rajamani P (2020). Iron oxide nanoparticle-induced hematopoietic and immunological response in rats. RSC Advances; 10(59): 35753-35764.
11. Gaharwar, U S, Paulraj R (2015). Iron oxide nanoparticles induced oxidative damage in peripheral blood cells of rat. Journal of Biomedical Science and Engineering; 8(04): 274-286.
12. Gheni, NA, Nanakali, N M, & Maulood, K A (2020). Protective effect of aqueous extract of neem (azadirachta indica) leaves against nicotine induced oxidative stress in a model of hyperlipidemia. Biochem. Cell. Arch; 20(1): 1407-1413.
13. Hagens WI, Oomen AG, de Jong WH, Casse FR, Sips AJ (2007). What do we need to know about the kinetic properties of nanoparticles in the body? Regulatory Toxicology and Pharmacology; 49(3): 217-229.
14. Idriss, H T, Naismith J H (2000). TNFα and the TNF receptor superfamily: Structure-function relationship (s). Microscopy Research and Technique; 50(3): 184-195.
15. Khanna P, Ong, C, Bay B H, Baeg G H (2015). Nanotoxicity: an interplay of oxidative stress, inflammation and cell death. Nanomaterials; 5(3): 1163-1180.
16. Kumar V, Abbas AK, Fausto N, Aster JC (2014). Robbins and Cotran: pathologic basis of disease, Ninth Ed. Saunders Elsevier, Philadelphia.
17. Li N, Sioutas C, Cho A, Schmitz D, Misra C, Sempf J, Nel A (2003). Ultrafine particulate pollutants induce oxidative stress and mitochondrial damage. Environmental Health Perspectives; 111(4): 455-460.
18. Liu G, Gao J, Ai H, Chen X (2013). Applications and potential toxicity of magnetic iron oxide nanoparticles. Small Journal 9(9–10): 1533–1545.
19. Missaoui WN, Arnold RD, Cummings BS (2018). Toxicological status of nanoparticles: what we know and what we don't know. Chemico-biological Interactions; 295: 1-12.
20. Morris J, Gonzales C B, De La Chapa J J, Cabang A B, Fountzilas C, Patel M Wargovich M J (2019). The highly pure neem leaf extract, SCNE, inhibits tumorigenesis in oral squamous cell carcinoma via disruption of pro-tumor inflammatory cytokines and cell signaling. Frontiers in Oncology; 9(890):1-14.
21. Oyagbemi A A, Omobowale T O, Ola-Davies O E, Adejumobi O A, Asenuga E R, Adeniji F K, Yakubu M A (2018). Protective effect of Azadirachta indica and vitamin E against arsenic acid-induced genotoxicity and apoptosis in rats. Journal of Dietary Supplements; 15(3): 251-268.
22. Pokhre B, Rijal S, Raut S, Pandeya A (2015). Investigations of antioxidant and antibacterial activity of leaf extracts of Azadirachta indica.African. Journal of Biotechnology; 14(46): 3159–3163.
23. Prashanth GK, Krishnaiah GM (2014). Chemical composition of the leaves of Azadirachta indica Linn (Neem). International Journal of Advancement in Engineering and Technology, Management and Applied Science; 1(3): 21-31.

24. Sithisarn P, Supabphol R, Gritsanapan W (2005). Antioxidant activity of Siamese neem tree (VP1209) Journal of Ethnopharmacology; 99(1):109–112.
25. Subapriya, R, Kumaraguruparan R, Nagini S (2006). Expression of PCNA, cytokeratin, Bcl-2 and p53 during chemoprevention of hamster buccal pouch carcinogenesis by ethanolic neem (Azadirachta indica) leaf extract. Clinical Biochemistry; 39(11): 1080-1087.
26. Sundarraj K, Manickam V, Raghunath A, Periyasamy M, Viswanathan MP, Perumal E (2017). Repeated Exposure to Iron oxide nanoparticles causes testicular toxicity in mice. Environmental Toxicology; 32(2): 594-608.
27. Verma G S, Nirmal N K, Gunpal D, Gupta H, Yadav M, Kumar N, John P J (2021). Intraperitoneal exposure of iron oxide nanoparticles causes dose-dependent toxicity in Wistar rats. Toxicology and Industrial Health; 37(12): 763-775.
28. Vinothini G, Manikandan P, Anandan R, Nagini S (2009). Chemoprevention of rat mammary carcinogenesis by Azadirachta indica leaf fractions: modulation of hormone status, xenobiotic-metabolizing enzymes, oxidative stress, cell proliferation and apoptosis. Food and Chemical Toxicology; 47(8): 1852-1863.
29. Yousef, MI, Abuzreda AA, Kamel MAN (2019a). Cardiotoxicity and lung toxicity in male rats induced by long-term exposure to iron oxide and silver nanoparticles. Experimental and Therapeutic Medicine; 18(6): 4329-4339.
30. Yousef, MI, Abuzreda AA, Kamel MAEN (2019b). Neurotoxicity and inflammation induced by individual and combined exposure to iron oxide nanoparticles and silver nanoparticles. Journal of Taibah University for Science; 13(1): 570-578.
31. Zhu MT, Feng WY, Wang B, Wang TC, Gu YQ, Wang M, Wang Y, Ouyang H, Zhao YL, Chai ZF (2008) Comparative study of pulmonary responses to nano- and submicron-sized ferric oxide in rats. Toxicology; 247(2–3):102–111.